

UT-801
 KUNS-1479
 HE(TH)97/19
 hep-ph/9712530

Quark and Lepton Mass Matrix in Asymptotically Non-Free Theory

Masako BANDO*, Joe SATO[†] and Koichi YOSHIOKA[‡]

**Aichi University, Aichi 470-02, Japan*

[†]Department of Physics, University of Tokyo, Tokyo 113, Japan

[‡]Department of Physics, Kyoto University, Kyoto 606-01, Japan

Abstract

We analyze fermion mass-matrix structure in an asymptotically non-free model with $4+\bar{1}$ generations. The texture at GUT scale is uniquely determined by supposing that the masses of heavy up-type quarks (top and charm) are realized as their infrared fixed point values. By assuming the $SO(10)$ GUT-like relations for Yukawa couplings in this model, this texture can explain all fermion masses and quark mixing with only one small parameter which is almost equal to the Cabibbo angle.

*E-mail address: bando@aichi-u.ac.jp

[†]E-mail address: joe@hep-th.phys.s.u-tokyo.ac.jp

[‡]E-mail address: yoshioka@gauge.scphys.kyoto-u.ac.jp

1 Introduction

The origin of fermion masses and mixing is one of the most important problems in constructing matter unification models. In the framework of the Minimal Supersymmetric Standard Model (MSSM) which is successful in attaining gauge coupling unification [1], there are lots of works to obtain fermion mass structure [2]. Especially a nice feature is found that the MSSM with $SU(5)$ -GUT relation is almost consistent with the observed bottom-tau mass ratio [3].

In the previous papers [4, 5], we investigated an extension of the MSSM having asymptotically non-free (ANF) property motivated by a possibility of dynamical gauge bosons. The difference between dynamical gauge bosons and elementary ones is the existence of the compositeness condition at some scale below which they behave as if they are asymptotically non-free gauge fields [6]. It is interesting to see whether or not the present standard gauge theory with ANF character preserves the above good predictions of the MSSM. As an example we consider the simplest case in which there are additional 2 extra generations, forming a generation-mirror generation pair (the 4th and anti-4th generations) with $SU(2)_W \times U(1)_Y$ invariant Dirac masses M . This is compatible with the constraints placed by the LEP measurements, namely the so-called Peskin-Takeuchi constraints [7]. Following Babu and Pati [8], we call this Extended Supersymmetric Standard Model (ESSM) hereafter.* In the ESSM three gauge couplings are also unified at the same scale as of the MSSM but with different unified coupling. An immediate consequence of the ESSM is that all three gauge couplings of $SU(3)_C$, $SU(2)_W$ and $U(1)_Y$, are ANF: they become larger as they are evolved up to coincide at the unification scale. We extended the analysis of the ESSM to see how the existence of the extra generations affects the running of the Yukawa couplings. We found that the bottom-tau mass ratio is nicely reproduced by taking GUT conditions different from those in the usual MSSM case [4] (see its quick review in section 2.3). Also we pointed out that the top quark mass is reproduced as an infrared fixed point (IRFP) prediction, which is almost insensitive to initial GUT conditions due to the ANF characters of gauge couplings [4, 5]. Such strong convergence of Yukawa couplings to their infrared fixed points is a common feature appearing in ANF theories [10]. We demonstrated how strongly the couplings are focused into their infrared fixed points in ANF theories as

*This ESSM had been intensively investigated in a context of a SUSY preon model [9].

well as the structure of the renormalization-group flows comparing the ESSM with the MSSM by concentrating on their infrared structure [5].

In the above analyses, we neglected the small Yukawa couplings of the first and second generations. However the existence of Yukawa couplings to the 4th and $\bar{4}$ th generations may affect on their structure in some way. In this paper we study the fermion masses of full 3 generations. As is well known, the ordinary fermion masses show typical hierarchical structures with small parameters $\sim O(10^{-(1-3)})$, which have to be introduced from the first as the GUT texture. In the ESSM case we have one more hierarchical factor; the ratio of the usual $SU(2)_W \times U(1)_Y$ breaking mass m and the invariant mass M ($m \ll M$). By making full use of the infrared fixed point structure and the hierarchical ratio m/M , we shall determine their textures at GUT scale.

In section 2 we make a quick summary of the present status of the fermion masses and mixing and of some features of our previous analysis in the ESSM. In section 3 we analyse the simplest case in which the invariant mass appears only in the 4th and $\bar{4}$ th fermions. It is found that the texture at GUT scale is uniquely determined if we impose that the masses of heavy up-type quarks (top and charm) are realized as their infrared fixed point values, together with $SO(10)$ GUT-like relations for Yukawa couplings. We will see that this texture reproduces all the fermion masses and quark mixing by introducing only one small parameter $\epsilon \sim 0.2$ which is almost equal to the Cabibbo angle. Concluding remarks and comments are made in section 4. Appendix A is devoted to the more complicated analysis in which texture is non-symmetric or more invariant masses M 's are included. We found none of them can reproduce the present experimental data of masses and mixing.

2 Fermion masses and mixing

2.1 Issues of fermion mass

The possible sources which determine fermion masses are

1. Texture of Yukawa matrix at GUT scale [11]: The GUT relations of Yukawa couplings are important to account for the hierarchical structure between generations. Although no rational basis is known to determine the intergenerational relationship, fermion masses show typical hierarchical structures quite

apparently. It may indicate the existence of a kind of generation quantum numbers. Actually there are many papers to explain hierarchical Yukawa couplings by assuming horizontal symmetry or using anomalous $U(1)$ or so [12], where we can make an active use of higher dimensional operators which effectively give very small Yukawa couplings. Anyhow it is important to determine the texture of the Yukawa matrix at GUT scale according to some yet unknown rule behind. We shall determine the texture phenomenologically assuming that some unknown mechanism yields hierarchical structure.

2. Running Yukawa couplings from GUT scale to weak scale: Once we fix the texture at GUT scale the renormalization-group equations (RGE) tell us the resultant Yukawa couplings at low-energy scale. Since the Yukawa couplings, except for those of third generation, are much smaller than the strength of gauge couplings (especially QCD coupling), usually renormalization effect mainly comes from QCD. The relative ratio between quark Yukawa couplings are not largely changed by RGE. The only important factor is the ratio of Yukawa couplings of quarks and leptons.
3. Mixing pattern of lightest Higgses: For the moment we treat the Higgs potential, and Higgs mixing (including $\tan\beta$) accordingly, as free parameters to be determined phenomenologically since we always encounter the well known fine-tuning problem.

For our later convenience, we summarize the masses of the present existing fermions at M_Z scale [13].

$$\begin{aligned}
m_u &\sim 2.33^{+0.42}_{-0.45} \text{ MeV}, & m_d &\sim 4.69^{+0.60}_{-0.66} \text{ MeV}, & m_e &\sim 0.486847 \text{ MeV}, \\
m_c &\sim 677^{+56}_{-61} \text{ MeV}, & m_s &\sim 93.4^{+11.8}_{-13.0} \text{ MeV}, & m_\mu &\sim 102.75 \text{ MeV}, \\
m_t &\sim 181 \pm 13 \text{ GeV}, & m_b &\sim 3.00 \pm 0.11 \text{ GeV}, & m_\tau &\sim 1.7467 \text{ GeV}.
\end{aligned} \tag{2.1}$$

2.2 Mixing angles

The observed values for the CKM matrix elements are [14]

$$|V_{\text{CKM}}| = \begin{pmatrix} 0.9745 - 0.9757 & 0.219 - 0.224 & 0.002 - 0.005 \\ 0.218 - 0.224 & 0.9736 - 0.9750 & 0.036 - 0.046 \\ 0.004 - 0.014 & 0.034 - 0.046 & 0.9989 - 0.9993 \end{pmatrix}, \tag{2.2}$$

which also indicates hierarchical structure;

$$\theta_{12} \sim \sin \theta_C \equiv \lambda \sim 0.22, \quad \theta_{23} \sim 0.04 \sim \lambda^2, \quad \theta_{13} \equiv x \sim (2-5) \times 10^{-3} \sim \lambda^{3-4}. \quad (2.3)$$

It is interesting to note the following relations between the mixing angles and the relevant mass eigenvalues (at M_Z);

- $\theta_{12} \sim 0.22$

$$\sqrt{m_u/m_c} = 0.051 \sim 0.067, \quad \sqrt{m_d/m_s} = 0.196 \sim 0.256, \quad (2.4)$$

- $\theta_{13} \sim 0.003$

$$\sqrt{m_u/m_t} = 0.003 \sim 0.004, \quad \sqrt{m_d/m_b} = 0.036 \sim 0.043, \quad (2.5)$$

- $\theta_{23} \sim 0.037$

$$\sqrt{m_c/m_t} = 0.056 \sim 0.066, \quad \sqrt{m_s/m_b} = 0.161 \sim 0.191, \quad (2.6)$$

where the mixing angles may be related to the ratios of the mass eigenvalues by taking the following down [15] and up [16] side mass matrices via seesaw mechanism, respectively,

$$m_D^{(12)} = \begin{matrix} & \begin{matrix} 1 & 2 \end{matrix} \\ \begin{matrix} 1 \\ 2 \end{matrix} & \begin{pmatrix} 0 & \lambda \\ \lambda & 1 \end{pmatrix} \end{matrix} \cdot m_s, \quad (2.7)$$

and

$$m_U^{(13)} = \begin{matrix} & \begin{matrix} 1 & 3 \end{matrix} \\ \begin{matrix} 1 \\ 3 \end{matrix} & \begin{pmatrix} 0 & x \\ x & 1 \end{pmatrix} \end{matrix} \cdot m_t. \quad (2.8)$$

However, the 2-3 mixing is too small compared with the mass ratio in either up or down sector. We need more complicated mechanism which may be the combination of mixing in both up and down sectors.

2.3 Fermion masses of 3rd generation in ESSM

Before going to the analysis on full fermion masses in the ESSM we make a quick review of the previous results [4, 5] of the third generation fermion masses.

The characteristic features of the ESSM are that, due to the ANF character, the Yukawa couplings approach to their infrared fixed points very rapidly and that the RGE effect of QCD on the quark enhances the down to lepton ratio much more with a factor $\sim (5 - 6)$ than the MSSM case (~ 3). One might think that the QCD enhancement will make it impossible to bring the low-energy bottom-tau mass ratio $R_{b/\tau}(M_Z)$ down to the experimental value ($1.6 \sim 1.8$) even with large Yukawa couplings (large $\tan \beta$). However, if we adopt the unification condition of an $SO(10)$ GUT with an 126-Higgs the extra enhancement from QCD is actually welcome since $R_{b/\tau}$ must be enhanced by a factor of $5 \sim 6$ to reproduce the experimental value of $R_{b/\tau}$,

$$Y_t(M_{\text{GUT}}) = Y_b(M_{\text{GUT}}) = \frac{1}{3}Y_\tau(M_{\text{GUT}}) \quad \rightarrow \quad R_{b/\tau}(M_Z) \sim \frac{5 \sim 6}{3}. \quad (2.9)$$

Another remarkable result is that due to the ANF gauge couplings the top and bottom Yukawa couplings are determined almost insensitively to their initial values fixed at GUT scale M_{GUT} . Indeed these Yukawa couplings reach to their fixed points, which are physically significant and provide us with reliable low-energy parameters. By using these fixed point solutions and the experimental value of $\alpha_3(1\text{TeV}) \sim 0.093$, we get for example,*

$$m_t(M_Z) \sim 178 \text{ GeV}, \quad m_b(M_Z) \sim 3.2 \text{ GeV}. \quad (2.10)$$

$$(\tan \beta \sim 58)$$

These values are certainly consistent with the experimental values [14].

3 Mass texture and IR fixed point

We consider the following ‘extended’ supersymmetric standard model with 5 generations; MSSM (3 generations) + 1 extra vector-like family ($4 + \bar{4}$). The matter content of this model is

$$Q_i, u_i, d_i, L_i, e_i, \quad i = 1, \dots, 4 \quad (3.1)$$

$$\bar{Q}, \bar{u}, \bar{d}, \bar{L}, \bar{e}, \quad (i = \bar{4}) \quad (3.2)$$

$$H, \bar{H}, \Phi. \quad (3.3)$$

*The tau-lepton Yukawa coupling generally has no infrared fixed point solution since it does not have the strong $SU(3)$ interaction. We then treat it as an input parameter and determine the value of $\tan \beta$ from the experimental value for $m_\tau(M_Z)$.

In addition to H, \bar{H} which are a pair of $SU(2)_W$ doublet Higgs fields, we have Φ , a (standard gauge group) singlet Higgs which yields masses for extra vector-like family. In this paper, we consider one Φ which gets vacuum expectation value of the order of TeV scale [17] by taking suitable soft breaking terms of Φ . In this situation, the superpotential becomes

$$\begin{aligned}
W = & \sum_{i,j=1,\dots,4} \mathbf{Y}_{u_{ij}} \epsilon_{ab} Q_i^a u_j \bar{H}^b + \mathbf{Y}_{d_{ij}} \epsilon_{ab} Q_i^a d_j H^b + \mathbf{Y}_{e_{ij}} \epsilon_{ab} L_i^a e_j H^b \\
& + Y_{\bar{u}} \bar{Q}_a \bar{u} H^a + Y_{\bar{d}} \bar{Q}_a \bar{d} \bar{H}^a + Y_{\bar{e}} \bar{L}_a \bar{e} \bar{H}^a \\
& + \sum_{i=1,\dots,4} Y_{Q_i} \Phi Q_i^a \bar{Q}_a + Y_{u_i} \Phi u_i \bar{u} + Y_{d_i} \Phi d_i \bar{d} + Y_{L_i} \Phi L_i^a \bar{L}_a + Y_{e_i} \Phi e_i \bar{e} + Y \Phi^3
\end{aligned} \tag{3.4}$$

where subscript i, j and a, b are indices of generation and $SU(2)_W$ respectively, and other indices are trivially contracted. With this superpotential, after $SU(2)_W \times U(1)_Y$ breaking, the forms of 5×5 fermion mass matrices are written as follows;

$$m_U = \begin{matrix} & u_{1R} & \cdots & u_{4R} & u_{\bar{4}R} \\ \begin{matrix} u_{1L} \\ \vdots \\ u_{4L} \\ u_{\bar{4}L} \end{matrix} & \begin{pmatrix} & & & \\ & \mathbf{Y}_{u_{ij}} v_u & & Y_{Q_i} V \\ & & & \\ & Y_{u_i} V & & Y_{\bar{u}} v_d \end{pmatrix} \end{matrix}, \tag{3.5}$$

$$m_D = \begin{matrix} & d_{1R} & \cdots & d_{4R} & d_{\bar{4}R} \\ \begin{matrix} d_{1L} \\ \vdots \\ d_{4L} \\ d_{\bar{4}L} \end{matrix} & \begin{pmatrix} & & & \\ & \mathbf{Y}_{d_{ij}} v_d & & Y_{Q_i} V \\ & & & \\ & Y_{d_i} V & & Y_{\bar{d}} v_u \end{pmatrix} \end{matrix}, \tag{3.6}$$

$$m_E = \begin{matrix} & e_{1R} & \cdots & e_{4R} & e_{\bar{4}R} \\ \begin{matrix} e_{1L} \\ \vdots \\ e_{4L} \\ e_{\bar{4}L} \end{matrix} & \begin{pmatrix} & & & \\ & \mathbf{Y}_{e_{ij}} v_d & & Y_{L_i} V \\ & & & \\ & Y_{e_i} V & & Y_{\bar{e}} v_u \end{pmatrix} \end{matrix}, \tag{3.7}$$

$$\langle H \rangle = \begin{pmatrix} v_d \\ 0 \end{pmatrix}, \quad \langle \bar{H} \rangle = \begin{pmatrix} 0 \\ v_u \end{pmatrix}, \quad \langle \Phi \rangle = V \tag{3.8}$$

where $u_{iL}, d_{iL}, (u_{\bar{4}R})^C$ and $(d_{\bar{4}R})^C$ are fermionic components of $SU(2)_W$ doublet quarks Q_i, \bar{Q} , and $(u_{iR})^C, (d_{iR})^C, u_{\bar{4}L}$ and $d_{\bar{4}L}$ are those of $SU(2)_W$ singlet quarks u_i, d_i, \bar{u} and \bar{d} , respectively.

3.1 Candidate for texture and IR fixed point

Before discussing realistic texture, we classify the types of texture which yield hierarchical masses, referring to their infrared behaviors. Since we know that the usual quark and lepton mass matrices show generally typical hierarchical structures, we first consider the dominant part of the matrices including only the 3rd, 4th and $\bar{4}$ th generations and then include less important contributions step by step. Hereafter for simplicity m, \bar{m} and M are used symbolically to represent $\mathbf{Y}_{f_{ij}}v_{u,d}, Y_{\bar{f}}v_{u,d}$ and $Y_{f_i}V$ ($f = u, d, e$) respectively since in our classification only the order of their masses are important ($m \ll M$). For the moment, let us restrict ourselves to the situation in which Yukawa couplings, $\mathbf{Y}_{f_{ij}}$, are symmetric (at GUT scale) and only the 4th generation couples to the $\bar{4}$ th generation forming an invariant mass term M . Analyses in general situations are performed in appendix A.

First let's consider the dominant matrices (the 3rd, 4th and $\bar{4}$ th generations). For $m \ll M$, after diagonalization at low energy, two of the three eigenvalues are of the order of M and one eigenvalue m_{33} is small compared with M . In order to get non-zero m_{33} there are three candidates for the textures classified by their determinants.

- case 1

$$\begin{array}{c} 3 \quad 4 \quad \bar{4} \\ 3 \quad \left(\begin{array}{ccc} m & & 0 \\ & & M \\ 0 & M & \end{array} \right), \quad \det_{3 \times 3} \sim M^2 m \end{array} \quad (3.9)$$

$$m_{33} \sim m \quad (3.10)$$

- case 2

$$\begin{array}{c} 3 \quad 4 \quad \bar{4} \\ 3 \quad \left(\begin{array}{ccc} 0 & m & 0 \\ m & & M \\ 0 & M & \bar{m} \end{array} \right), \quad \det_{3 \times 3} \sim m^2 \bar{m} \end{array} \quad (3.11)$$

$$m_{33} \sim \left(\frac{m \bar{m}}{M^2} \right) m \quad (3.12)$$

- case 3

$$\begin{array}{c} 3 \quad 4 \quad \bar{4} \\ \begin{array}{c} 3 \\ 4 \\ \bar{4} \end{array} \begin{pmatrix} 0 & m & 0 \\ m & m & M \\ 0 & M & 0 \end{pmatrix}, \quad \det_{3 \times 3} \sim 0 \end{array} \quad (3.13)$$

$$m_{33} \sim \text{radiatively induced} \quad (3.14)$$

where, and hereafter, element “0” means that it should be exactly zero at GUT scale in contrast to the notation “blank” which can be either zero or not. For the case 3, the determinant of this texture is zero. However, this type of matrix induces appreciable non-zero Y_{33} element via radiative corrections and the resultant low-energy determinant (and eigenvalue m_{33}) cannot be neglected.

Next, we include the second generation and consider 4×4 matrix. In order to get hierarchical mass eigenvalue after diagonalization, $m_{22} \ll m_{33} \ll M$, it is needed to realize the hierarchical determinants $\det_{4 \times 4} / \det_{3 \times 3} \ll m_{33}$. Then the resultant 4×4 textures which realize this hierarchical structure are found to be the followings;

- case 1

There are two distinct types of texture.

- type A

$$\begin{array}{c} 2 \quad 3 \quad 4 \quad \bar{4} \\ \begin{array}{c} 2 \\ 3 \\ 4 \\ \bar{4} \end{array} \begin{pmatrix} 0 & 0 & m & 0 \\ 0 & m & & 0 \\ m & & & M \\ 0 & 0 & M & \bar{m} \end{pmatrix}, \quad \det_{4 \times 4} \sim m^3 \bar{m} \end{array} \quad (3.15)$$

$$m_{22} \sim \left(\frac{m \bar{m}}{M^2} \right) m \quad (3.16)$$

- type B

$$\begin{array}{c} 2 \quad 3 \quad 4 \quad \bar{4} \\ \begin{array}{c} 2 \\ 3 \\ 4 \\ \bar{4} \end{array} \begin{pmatrix} 0 & 0 & m & 0 \\ 0 & m & & 0 \\ m & & m & M \\ 0 & 0 & M & 0 \end{pmatrix}, \quad \det_{4 \times 4} \sim 0 \end{array} \quad (3.17)$$

$$m_{22} \sim \text{radiatively induced} \quad (3.18)$$

Note that in these textures the 3rd generation is almost decoupled from the other generations. On the contrary, these textures are of the same forms as those of case 2 and 3 ((3.11) and (3.13)) which are used for the 2nd, 4th and $\bar{4}$ th generations to get non-zero m_{22} and so this small eigenvalue m_{22} is strongly affected by the existence of the 4th and $\bar{4}$ th generations.

- case 2, 3

We found that there is essentially no candidate in these cases.

One might think that the following texture reproduces non-zero eigenvalue m_{22} radiatively.

$$\begin{array}{c} 2 \quad 3 \quad 4 \quad \bar{4} \\ \begin{array}{c} 2 \\ 3 \\ 4 \\ \bar{4} \end{array} \begin{pmatrix} 0 & 0 & m & 0 \\ 0 & 0 & m & 0 \\ m & m & m & M \\ 0 & 0 & M & \end{pmatrix}, \quad \det_{4 \times 4} \sim 0 \end{array} \quad (3.19)$$

However, in this texture the second and third generations have the same structure. Therefore this matrix has at most rank 3 and yields almost zero eigenvalue for m_{22} even when all the induced Yukawa couplings are included.

There are two more candidates for the texture having hierarchical mass structure.

$$\begin{array}{c} 2 \quad 3 \quad 4 \quad \bar{4} \\ \begin{array}{c} 2 \\ 3 \\ 4 \\ \bar{4} \end{array} \begin{pmatrix} m & 0 & & 0 \\ 0 & 0 & m & 0 \\ & m & & M \\ 0 & 0 & M & \bar{m} \end{pmatrix}, \quad \det_{4 \times 4} \sim m^3 \bar{m} \end{array} \quad (3.20)$$

$$\begin{array}{c} 2 \quad 3 \quad 4 \quad \bar{4} \\ \begin{array}{c} 2 \\ 3 \\ 4 \\ \bar{4} \end{array} \begin{pmatrix} m & 0 & & 0 \\ 0 & 0 & m & 0 \\ & m & m & M \\ 0 & 0 & M & 0 \end{pmatrix}, \quad \det_{4 \times 4} \sim 0 \end{array} \quad (3.21)$$

However, (3.20) and (3.21) coincide with (3.15) and (3.17) by changing the label of the generation ($2 \leftrightarrow 3$). We do not consider these types of texture.*

In conclusion, we have two candidates (3.15) and (3.17) which reproduce hierarchical mass structure between the second and third generations of the up and down sectors.

In addition to the difference of the mass eigenvalues between type A and B, another remarkable difference exists between these two types of texture. As we have already mentioned, it is the infrared behavior of Yukawa couplings that is characteristic to this ANF model. So long as we restrict ourselves to the third generation, two textures have the same infrared structures (figure 1 and 2): the

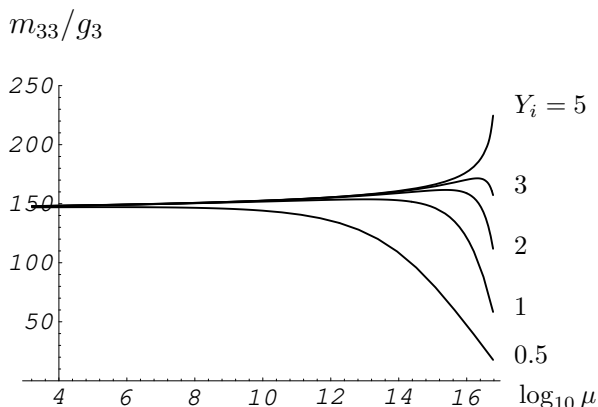


Figure 1: Typical behavior of m_{33} in the type A texture.

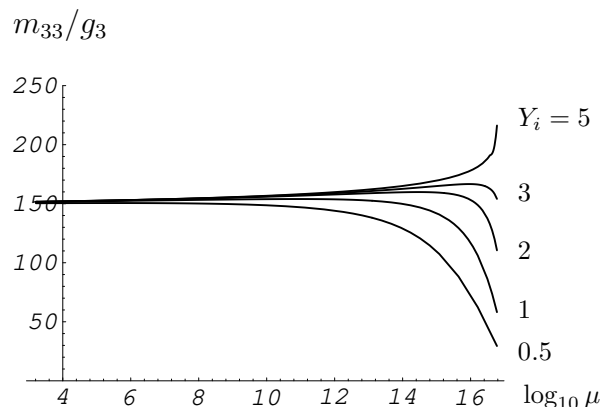


Figure 2: Typical behavior of m_{33} in the type B texture.

(In the above figures, all the non-zero Yukawa couplings at GUT scale are taken to be the same value Y_i .)

Yukawa coupling Y_{33} sits almost on its infrared fixed point at low energy in both cases. However, the infrared behaviors of the eigenvalues of the second generation are quite different. For the type A texture the resultant eigenvalue m_{22} (see (3.16)) is obtained from the tree-level Yukawa couplings (and VEVs whose order are assumed) and therefore can be regarded as an infrared fixed point value (figure 3). On the other hand, for the type B texture the eigenvalue m_{22} is induced radiatively by

*Strictly speaking, we cannot exchange the generation label ($2 \leftrightarrow 3$) when we use one of (3.15) and (3.17) for up-quark sector and one of (3.20) and (3.21) for down-quark sector and vice versa, for example. This case yields a large mixing angle between generations which is experimentally excluded.

renormalization procedure and does not reach its theoretical infrared fixed point value at low energy (figure 4).

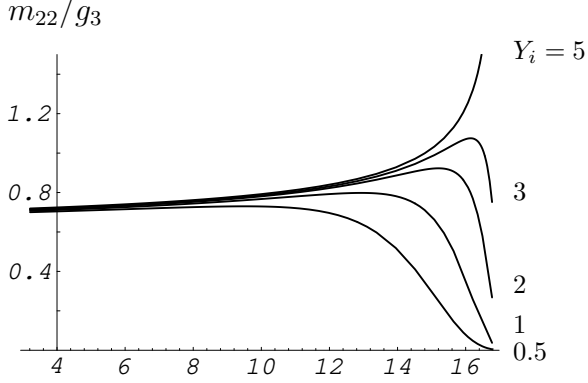


Figure 3: Typical behavior of m_{22} in the type A texture.

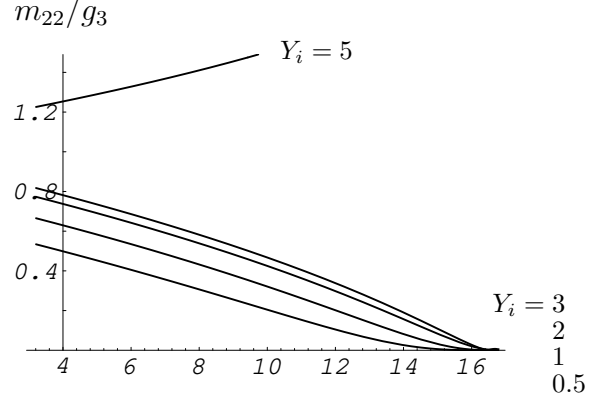


Figure 4: Typical behavior of m_{22} in the type B texture.

3.2 Texture for mass matrix

Next, we argue which texture can be used for the quark and lepton sectors. From the above discussions we have learned that the type A texture provides us with a mechanism in which we can make a full use of infrared fixed points. We see from figure 5 that the typical value of the hierarchical factor $\frac{m\bar{m}}{M^2}$ (see (3.16)) in the type A texture is generally $1/100$ or less, and that this factor becomes smaller for larger $\tan\beta$. It is far smaller than the observed bottom to strange ratio ($\sim 1/30$). Therefore we do not use the type A texture for the down-quark and charged lepton sectors, but adopt the type B texture. On the other hand, the hierarchical factor of the up-quark sector, top and charm ratio ($\sim 1/250$), is much smaller than the ratio of bottom and strange. We can adopt the type A mass texture for the up-quark sector. Note that in the type A texture the masses of heavy quarks (top and charm) are given by the infrared fixed point values for Yukawa couplings which are almost insensitive to their initial values at M_{GUT} .

Once we fix the texture for the up and down/lepton sectors, we can estimate the quark and lepton masses. However there arises two difficulties in reproducing hierarchical structures both in up and down sectors. First, the top and bottom Yukawa couplings reach their infrared fixed point values, which requires large $\tan\beta$ scenario. This large $\tan\beta$ scenario makes hierarchical factor for the up-sector much

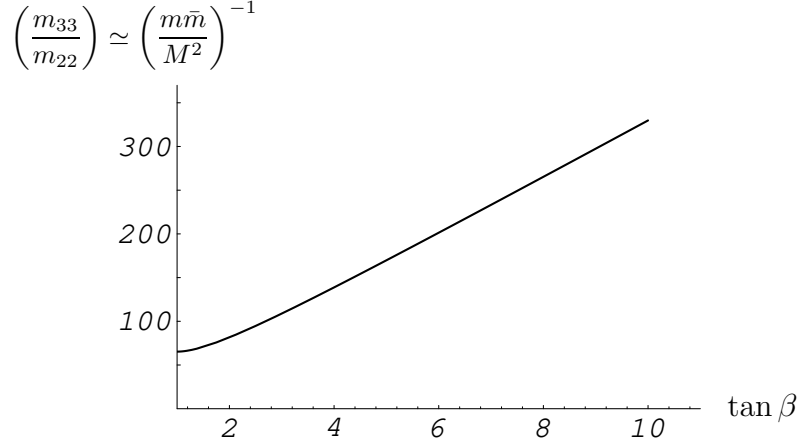


Figure 5: Typical behavior of hierarchical factor in the type A texture ($M = 1$ TeV).

smaller than the actual value of the ratio of top and charm (see figure 5). Second, the ratio of the eigenvalues, m_{33}/m_{22} , at low energy scale is found to be at least 100 in the type B texture (figure 6). Thus some improvement must be made to overcome

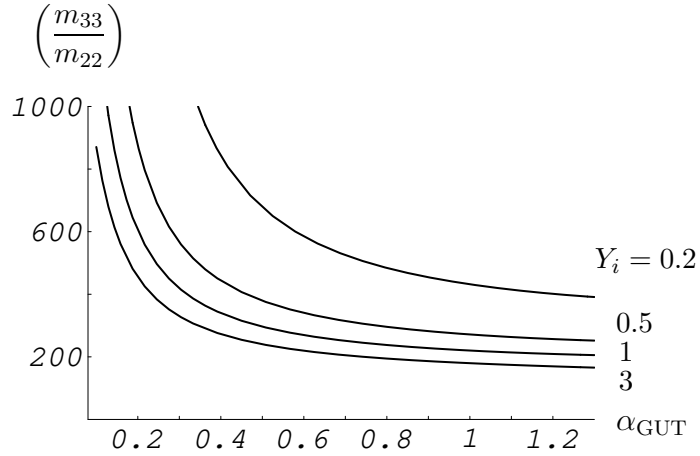


Figure 6: Typical behavior of hierarchical factor in the type B texture.

the above mismatches. We found that we can solve both difficulties by introducing only one parameter ϵ and attaching it to bottom quark Yukawa coupling.[†] We

[†]Even when ϵ parameter is introduced the type A texture cannot be used for the down/lepton sector because their non-zero Y_{44} elements contribute to the beta-function of top Yukawa coupling

finally found that the following mass texture for quark and lepton at GUT scale can reproduce the low-energy experimental values of the fermion masses.

$$m_U = \begin{array}{c} 2 \quad 3 \quad 4 \quad \bar{4} \\ \begin{array}{c} 2 \\ 3 \\ 4 \\ \bar{4} \end{array} \begin{pmatrix} 0 & 0 & m & 0 \\ 0 & m & & 0 \\ m & & & M \\ 0 & 0 & M & \bar{m} \end{pmatrix} \end{array}, \quad (3.22)$$

$$m_D = \begin{array}{c} 2 \quad 3 \quad 4 \quad \bar{4} \\ \begin{array}{c} 2 \\ 3 \\ 4 \\ \bar{4} \end{array} \begin{pmatrix} 0 & 0 & m & 0 \\ 0 & \epsilon m & 0 & 0 \\ m & 0 & m & M \\ 0 & 0 & M & 0 \end{pmatrix} \end{array}, \quad (3.23)$$

$$m_E = \begin{array}{c} 2 \quad 3 \quad 4 \quad \bar{4} \\ \begin{array}{c} 2 \\ 3 \\ 4 \\ \bar{4} \end{array} \begin{pmatrix} 0 & 0 & 3m & 0 \\ 0 & 3\epsilon m & 0 & 0 \\ 3m & 0 & 3m & M \\ 0 & 0 & M & 0 \end{pmatrix} \end{array}, \quad (3.24)$$

where we use the Higgs field of 126 (45) representation of $SO(10)$ ($SU(5)$) so that the boundary conditions in the down/lepton sector may correctly reproduce the observed b/τ (or s/μ) ratio as noted in the previous section. In this texture, all quark Yukawa couplings except for \mathbf{Y}_{d33} converge to their infrared fixed points independently of their initial values at GUT scale. Within this approximation, this texture leads the following low-energy prediction of fermion masses;[‡]

$$\begin{aligned} M_{\text{GUT}} &\sim 5.3 \times 10^{16} \text{ GeV}, & \alpha_{\text{GUT}} &\sim 0.3, & \epsilon &\sim 0.2, \\ M_{\text{SUSY}} &\sim 1 \text{ TeV}, & \tan \beta &\sim 20, & V &\sim 3 \text{ TeV}, \end{aligned} \quad (3.25)$$

$$\begin{aligned} \Rightarrow \quad m_t &\sim 180 \text{ GeV}, & m_c &\sim 1.0 \text{ GeV}, \\ m_b &\sim 3.1 \text{ GeV}, & m_s &\sim 0.081 \text{ GeV}, & (\text{at } M_Z) \\ m_\tau &\sim 1.75 \text{ GeV}, & m_\mu &\sim 0.103 \text{ GeV}. \end{aligned} \quad (3.26)$$

The result is in good agreement with the present experimental values.

and make its infrared fixed point value far smaller than the experimental one.

[‡]For simplicity, we set the blanks in m_U (3.22) to be zeros.

3.3 CKM mixing angles

Encouraged by the successful results of the texture in the previous section, we finally consider full mass matrix including quark mixing angles. This may be done by introducing hierarchically very small Yukawa couplings. As noted in section 2, 1-3 quark mixing is well described by the 1-3 mixing in the up-quark sector and 1-2 quark mixing by the 1-2 mixing in the down-quark sector. Therefore the eigenvalue m_{11} for up- (down-) quark sector can be automatically reproduced by introducing a small mixing $\mathbf{Y}_{u_{13}}$ ($\mathbf{Y}_{d_{12}}$) into our texture. The problem arises in 2-3 quark mixing for which the usual seesaw-type relation between mixing angle and eigenvalues is not successful. Fortunately enough, however, in our extended model, the mass eigenvalues for the second generation can be properly reproduced by mixing with extra vector-like generations. Therefore the 2-3 mixing parameter can be treated independently of the 2-2 mass eigenvalue so far as it does not affect m_{22} very strongly. We can thus adopt the following 3×3 matrix for the ordinary quark sector in which the CKM mixing angles may correctly reproduced.

$$(m_U)_{3 \times 3} = \begin{matrix} & \begin{matrix} 1 & 2 & 3 \end{matrix} \\ \begin{matrix} 1 \\ 2 \\ 3 \end{matrix} & \left(\begin{array}{ccc} & & \\ & & \epsilon^l \\ \epsilon^l & & 1 \end{array} \right), \end{matrix} \quad (3.27)$$

$$(m_D)_{3 \times 3} = \begin{matrix} & \begin{matrix} 1 & 2 & 3 \end{matrix} \\ \begin{matrix} 1 \\ 2 \\ 3 \end{matrix} & \left(\begin{array}{ccc} & & \\ & \epsilon^m & \\ \epsilon^m & & \epsilon^n \\ & \epsilon^n & \epsilon \end{array} \right). \end{matrix} \quad (3.28)$$

The down-quark (and charged lepton) sector is just the Fritzsch type of texture [18] in which the mass of the second generation induced by seesaw mechanism is much smaller than “tree-level” one, which now comes from mixing with the 4th and $\bar{4}$ th generations. At this point, note that ϵ parameter in the texture in the previous section happens to be just the same value as the Cabibbo mixing angle (see (3.25)) for explaining all hierarchies in the second and third generations of quarks and leptons. Therefore it is not necessary to introduce any small mixing parameter

other than ϵ .

m	$ V_{us} $	n	$ V_{cb} $	l	$ V_{ub} $	m_u
3	0.6	2	0.17	3	0.008	~ 32 MeV
4	0.27	3	0.035	4	0.002	~ 1.3 MeV
5	0.06	4	0.007	5	0.0003	~ 0.5 MeV

(3.29)

m	n	$ V_{ub} $	m	n	$ V_{ub} $	m	n	$ V_{ub} $
3	2	0.044	4	2	0.01	5	2	0.002
3	3	0.009	4	3	0.002	5	3	0.0004
3	4	0.002	4	4	0.0004	5	4	0.0001

(3.30)

After all, there is a reasonable 5×5 GUT-scale texture which explains the experimental values of the CKM mixing angle and we can see that this texture is actually the only possibility left under this situation.

$$m_U \simeq \begin{matrix} & \begin{matrix} 1 & 2 & 3 & 4 & \bar{4} \end{matrix} \\ \begin{matrix} 1 \\ 2 \\ 3 \\ 4 \\ \bar{4} \end{matrix} & \begin{pmatrix} 0 & 0 & \epsilon^4 m & 0 & 0 \\ 0 & 0 & 0 & m & 0 \\ \epsilon^4 m & 0 & m & 0 & 0 \\ 0 & m & 0 & 0 & M \\ 0 & 0 & 0 & M & \bar{m} \end{pmatrix} \end{matrix}, \quad (3.31)$$

$$m_D \simeq \begin{matrix} & \begin{matrix} 1 & 2 & 3 & 4 & \bar{4} \end{matrix} \\ \begin{matrix} 1 \\ 2 \\ 3 \\ 4 \\ \bar{4} \end{matrix} & \begin{pmatrix} 0 & \epsilon^4 m & 0 & 0 & 0 \\ \epsilon^4 m & 0 & \epsilon^3 m & m & 0 \\ 0 & \epsilon^3 m & \epsilon m & 0 & 0 \\ 0 & m & 0 & m & M \\ 0 & 0 & 0 & M & 0 \end{pmatrix} \end{matrix}, \quad (3.32)$$

$$m_E \simeq \begin{matrix} & \begin{matrix} 1 & 2 & 3 & 4 & \bar{4} \end{matrix} \\ \begin{matrix} 1 \\ 2 \\ 3 \\ 4 \\ \bar{4} \end{matrix} & \begin{pmatrix} 0 & 3\epsilon^4 m & 0 & 0 & 0 \\ 3\epsilon^4 m & 0 & 3\epsilon^3 m & 3m & 0 \\ 0 & 3\epsilon^3 m & 3\epsilon m & 0 & 0 \\ 0 & 3m & 0 & 3m & M \\ 0 & 0 & 0 & M & 0 \end{pmatrix} \end{matrix}, \quad (3.33)$$

$$\begin{aligned} \Rightarrow \quad & m_u \sim 2.9 \text{ MeV}, & m_d \sim 4.3 \text{ MeV}, & m_e \sim 0.6 \text{ MeV}, \\ & m_c \sim 1.0 \text{ GeV}, & m_s \sim 0.089 \text{ GeV}, & m_\mu \sim 0.104 \text{ GeV}, \\ & m_t \sim 180 \text{ GeV}, & m_b \sim 3.1 \text{ GeV}, & m_\tau \sim 1.75 \text{ GeV}, \end{aligned} \quad (3.34)$$

$$|V_{\text{CKM}}| \simeq \begin{pmatrix} 0.974 & 0.228 & 0.0037 \\ 0.228 & 0.973 & 0.039 \\ 0.005 & 0.039 & 0.999 \end{pmatrix}. \quad (3.35)$$

These values are almost consistent with the experimental ones.

4 Summary and Conclusion

We have investigated the fermion mass matrix structure at GUT scale in an asymptotically non-free theory with $4 + \bar{1}$ generations. The characteristic feature of our model is that the couplings converge to their infrared fixed points very quickly. By making a full use of the behavior of the couplings we determined the fermion mass matrix at GUT scale uniquely.

We have found that: 1) We can understand the charm quark mass as well as the top quark mass in terms of their infrared fixed point values. It is interesting that the hierarchical factor of the top and charm ratio comes from the existence of the 4th and $\bar{4}$ th generations. Also we should like to note that the Yukawa couplings of $Y_{24}(Y_{42})$ reach their infrared fixed points with considerable strength. This indicates that the second generation is strongly coupled with the extra generations. 2) Though the masses of the other lighter quarks are not related to the infrared structure of the ANF character, we can determine their mass texture almost uniquely by introducing only one small parameter. It is interesting that this small parameter happens to be equal to the Cabibbo mixing angle. In the down-quark texture the resultant strange-quark eigenvalue is suppressed by the existence of the extra generations in spite of the appreciable large induced Yukawa coupling Y_{22} . 3) As for the lepton masses, they are reproduced quite successfully by assuming that the relevant Higgs field belongs to 126 representation of $SO(10)$. This is in a remarkable contrast to the case of the MSSM in which, as is seen from the Georgi-Jarlskog type of texture [19], we have to assume that the relevant Higgs field must be the mixture of 10 and 126 representations.

It was essential for us to understand the heavier fermion masses as their IR fixed point values that not only the SUSY breaking scale but also the invariant masses

of the extra generations are of the order of TeV scale. This fact implies that when SUSY is discovered the extra generations may be also found. By a muon collider [20], especially the extra generations may be explored easily since in our model the second generation couples strongly to the extra generations.

Acknowledgements

We would like to thank to T. Kugo and N. Maekawa for many helpful discussions and variable comments. M. B. is supported in part by the Grant-in Aid for Scientific Research No. 09640375.

Appendix A More complex cases

In this appendix, we briefly present our analysis on two more complex cases: in one case, more than two generations couple to the $\bar{4}$ th generation via invariant mass terms and in the other case the form of texture is non-symmetric.

1 More than two M 's

Let us make the classification of hierarchical textures, following the analysis in section 3. First, we consider 3×3 texture. In addition to three textures argued in section 3 ((3.9), (3.11), (3.13)), there are two types of texture which provide non-zero eigenvalue m_{33} .

- case 4

$$\begin{array}{c} 3 \quad 4 \quad \bar{4} \\ 3 \quad \left(\begin{array}{ccc} 0 & m & M' \\ m & 0 & M \\ M' & M & 0 \end{array} \right), \quad \det_{3 \times 3} \sim MM'm \\ 4 \\ \bar{4} \end{array} \quad (A.1)$$

$$m_{33} \sim \left(\frac{M'}{M} \right) m \quad (A.2)$$

- case 5

$$\begin{array}{c} 3 \quad 4 \quad \bar{4} \\ \begin{array}{c} 3 \\ 4 \\ \bar{4} \end{array} \begin{pmatrix} 0 & 0 & M' \\ 0 & m & M \\ M' & M & \end{pmatrix}, \quad \det_{3 \times 3} \sim M'^2 m \end{array} \quad (\text{A.3})$$

$$m_{33} \sim \left(\frac{M'}{M} \right)^2 m \quad (\text{A.4})$$

From the above two textures, we get three types of texture which produce the hierarchical mass eigenvalues, $m_{22} \ll m_{33} \ll M, M'$ at low energy without small parameter ϵ in addition to the type A and B textures obtained in section 3.

- case 4

- type C

$$\begin{array}{c} 2 \quad 3 \quad 4 \quad \bar{4} \\ \begin{array}{c} 2 \\ 3 \\ 4 \\ \bar{4} \end{array} \begin{pmatrix} 0 & m & m & M' \\ m & & m & 0 \\ m & m & & M \\ M' & 0 & M & \end{pmatrix} \end{array} \quad (\text{A.5})$$

- case 5

- type D

$$\begin{array}{c} 2 \quad 3 \quad 4 \quad \bar{4} \\ \begin{array}{c} 2 \\ 3 \\ 4 \\ \bar{4} \end{array} \begin{pmatrix} 0 & m & 0 & M' \\ m & m & 0 & 0 \\ 0 & 0 & m & M \\ M' & 0 & M & \end{pmatrix} \end{array} \quad (\text{A.6})$$

- type E

$$\begin{array}{c} 2 \quad 3 \quad 4 \quad \bar{4} \\ \begin{array}{c} 2 \\ 3 \\ 4 \\ \bar{4} \end{array} \begin{pmatrix} & m & & M' \\ m & 0 & m & 0 \\ & m & m & M \\ M' & 0 & M & \end{pmatrix} \end{array} \quad (\text{A.7})$$

Then we consider the realistic mass texture of quark and lepton. One can easily see that all the above types of texture have hierarchical factors of order $1/100$ or less. Therefore we must also introduce a (small) parameter ϵ to obtain the hierarchy in the down-quark and/or lepton sector. On the other hand, we can get the hierarchy in the up-quark sector from any one of five textures. As mentioned in section 3, we adopt the type A texture for up-quark sector by making an active use of the infrared fixed point structure which is characteristic feature of this ANF model. Note that due to the $SO(10)$ -like GUT relations for Yukawa couplings to singlet Higgs if we adopt the textures of type C–E for the down and lepton sectors we have to add M' to the up-quark texture (the type A texture). These M' 's change the determinant and so spoil the hierarchical structure of the type A texture. Therefore we also have to include small ϵ parameter in the invariant mass term M' . Taking into account all issues discussed until now, we searched the realistic textures of quark and lepton at GUT scale. However, we found no candidate except for the one obtained in section 3 to reproduce the present experimental data of hierarchical mass eigenvalues.

2 Non-symmetric texture

Until now, we implicitly take the textures to be symmetric. Another more general analysis is to consider non-symmetric type of texture. However, general analysis is too complex and is not so physically meaningful. Therefore we suppose the up-type texture to be the type A likewise. We made numerical analysis on the types of 4×4 texture for the down-quark and charged lepton sectors which reproduce the hierarchical mass ratios $c/t, s/b$ and μ/τ etc. without small parameter ϵ . Even in this situation, we found no realistic candidate except for the one obtained in section 3.

Appendix B The beta-functions

We present the 2-loop beta-functions for gauge couplings of $SU(3)_C \times SU(2)_W \times U(1)_Y$ and the 1-loop ones for Yukawa couplings. We here neglect the CP phase which does not affect the numerical results. The evolution of gauge coupling con-

stants is given by

$$\frac{dg_i}{dt} = b_i \frac{g_i^3}{16\pi^2} + \frac{g_i^3}{(16\pi^2)^2} \left[\sum_j b_{ij} g_j^2 - \sum_{a=u,d,e} c_{ia} \left(\text{Tr}(\mathbf{Y}_a^T \mathbf{Y}_a) + Y_{\bar{a}}^2 \right) - \sum_{k=1}^4 \sum_{X=Q,u,d,L,e} d_{iX} Y_{X_k}^2 \right], \quad (\text{B.1})$$

where $b_i = (10.6, 5, 1)$ for $U(1)_Y$ (in a GUT normalization), $SU(2)_W$ and $SU(3)_C$ respectively, and

$$b_{ij} = \begin{pmatrix} 977/75 & 39/5 & 88/3 \\ 13/5 & 53 & 40 \\ 11/3 & 15 & 178/3 \end{pmatrix}, \quad (\text{B.2})$$

$$c_{ia} = \begin{pmatrix} 26/5 & 14/5 & 18/5 \\ 6 & 6 & 2 \\ 4 & 4 & 0 \end{pmatrix}, \quad (\text{B.3})$$

$$d_{iX} = \begin{pmatrix} 2/5 & 32/5 & 8/5 & 6/5 & 12/5 \\ 6 & 3 & 3 & 2 & 0 \\ 4 & 2 & 2 & 0 & 0 \end{pmatrix}. \quad (\text{B.4})$$

The beta-functions for Yukawa couplings in the superpotential (3.4) are given as follows.

$$\frac{d\mathbf{Y}_{a_{ij}}}{dt} = \frac{1}{16\pi^2} \beta_{a_{ij}}, \quad (a = u, d, e) \quad (\text{B.5})$$

$$\frac{dY_{\bar{a}}}{dt} = \frac{1}{16\pi^2} \beta_{\bar{a}}, \quad (a = u, d, e) \quad (\text{B.6})$$

$$\frac{dY_{X_i}}{dt} = \frac{1}{16\pi^2} \beta_{X_i}, \quad (X = Q, u, d, L, e) \quad (\text{B.7})$$

$$\frac{dY}{dt} = \frac{1}{16\pi^2} \beta_Y, \quad (\text{B.8})$$

$$\begin{aligned} \beta_{u_{ij}} &= \mathbf{Y}_{u_{ij}} \left[3\text{Tr}(\mathbf{Y}_u^T \mathbf{Y}_u) + 3Y_{\bar{d}}^2 + Y_{\bar{e}}^2 - \frac{16}{3}g_3^2 - 3g_2^2 - \frac{13}{15}g_1^2 \right] \\ &+ \left(3\mathbf{Y}_u \mathbf{Y}_u^T \mathbf{Y}_u + \mathbf{Y}_u \mathbf{Y}_d^T \mathbf{Y}_d \right)_{ij} + \sum_k \left(\mathbf{Y}_{u_{kj}} Y_{Q_i} Y_{Q_k} + \mathbf{Y}_{u_{ik}} Y_{u_k} Y_{u_j} \right), \quad (\text{B.9}) \end{aligned}$$

$$\begin{aligned} \beta_{d_{ij}} &= \mathbf{Y}_{d_{ij}} \left[\text{Tr}(3\mathbf{Y}_d^T \mathbf{Y}_d + \mathbf{Y}_e^T \mathbf{Y}_e) + 3Y_{\bar{u}}^2 - \frac{16}{3}g_3^2 - 3g_2^2 - \frac{7}{15}g_1^2 \right] \\ &+ \left(3\mathbf{Y}_d \mathbf{Y}_d^T \mathbf{Y}_d + \mathbf{Y}_d \mathbf{Y}_u^T \mathbf{Y}_u \right)_{ij} + \sum_k \left(\mathbf{Y}_{d_{kj}} Y_{Q_i} Y_{Q_k} + \mathbf{Y}_{d_{ik}} Y_{d_k} Y_{d_j} \right), \quad (\text{B.10}) \end{aligned}$$

$$\begin{aligned}\beta_{e_{ij}} &= \mathbf{Y}_{e_{ij}} \left[\text{Tr}(3\mathbf{Y}_d^T \mathbf{Y}_d + \mathbf{Y}_e^T \mathbf{Y}_e) + 3Y_{\bar{u}}^2 - 3g_2^2 - \frac{9}{5}g_1^2 \right] \\ &\quad + 3 \left(\mathbf{Y}_e \mathbf{Y}_e^T \mathbf{Y}_e \right)_{ij} + \sum_k \left(\mathbf{Y}_{e_{kj}} Y_{L_i} Y_{L_k} + \mathbf{Y}_{e_{ik}} Y_{e_k} Y_{e_j} \right),\end{aligned}\quad (\text{B.11})$$

$$\beta_{\bar{u}} = Y_{\bar{u}} \left[\text{Tr}(3\mathbf{Y}_d^T \mathbf{Y}_d + \mathbf{Y}_e^T \mathbf{Y}_e) + 6Y_{\bar{u}}^2 + Y_d^2 + \sum_i (Y_{Q_i}^2 + Y_{u_i}^2) - \frac{16}{3}g_3^2 - 3g_2^2 - \frac{13}{15}g_1^2 \right], \quad (\text{B.12})$$

$$\beta_{\bar{d}} = Y_{\bar{d}} \left[\text{Tr}(3\mathbf{Y}_u^T \mathbf{Y}_u) + Y_{\bar{u}}^2 + 6Y_{\bar{d}}^2 + Y_{\bar{e}}^2 + \sum_i (Y_{Q_i}^2 + Y_{d_i}^2) - \frac{16}{3}g_3^2 - 3g_2^2 - \frac{7}{15}g_1^2 \right], \quad (\text{B.13})$$

$$\beta_{\bar{e}} = Y_{\bar{e}} \left[\text{Tr}(3\mathbf{Y}_u^T \mathbf{Y}_u) + 3Y_{\bar{d}}^2 + 4Y_{\bar{e}}^2 + \sum_i (Y_{L_i}^2 + Y_{e_i}^2) - 3g_2^2 - \frac{9}{5}g_1^2 \right], \quad (\text{B.14})$$

$$\begin{aligned}\beta_{Q_i} &= Y_{Q_i} \left[Y_{\bar{u}}^2 + Y_{\bar{d}}^2 + \sum_j (8Y_{Q_j}^2 + 3Y_{u_j}^2 + 3Y_{d_j}^2 + 2Y_{L_j}^2 + Y_{e_j}^2) + Y^2 \right. \\ &\quad \left. - \frac{16}{3}g_3^2 - 3g_2^2 - \frac{1}{15}g_1^2 \right] + \sum_k Y_{Q_k} \left(\mathbf{Y}_u^T \mathbf{Y}_u + \mathbf{Y}_d^T \mathbf{Y}_d \right)_{ik},\end{aligned}\quad (\text{B.15})$$

$$\begin{aligned}\beta_{u_i} &= Y_{u_i} \left[2Y_{\bar{u}}^2 + \sum_j (6Y_{Q_j}^2 + 5Y_{u_j}^2 + 3Y_{d_j}^2 + 2Y_{L_j}^2 + Y_{e_j}^2) + Y^2 \right. \\ &\quad \left. - \frac{16}{3}g_3^2 - \frac{16}{15}g_1^2 \right] + \sum_k 2Y_{u_k} \left(\mathbf{Y}_u^T \mathbf{Y}_u \right)_{ik},\end{aligned}\quad (\text{B.16})$$

$$\begin{aligned}\beta_{d_i} &= Y_{d_i} \left[2Y_{\bar{d}}^2 + \sum_j (6Y_{Q_j}^2 + 3Y_{u_j}^2 + 5Y_{d_j}^2 + 2Y_{L_j}^2 + Y_{e_j}^2) + Y^2 \right. \\ &\quad \left. - \frac{16}{3}g_3^2 - \frac{4}{15}g_1^2 \right] + \sum_k 2Y_{d_k} \left(\mathbf{Y}_d^T \mathbf{Y}_d \right)_{ik},\end{aligned}\quad (\text{B.17})$$

$$\begin{aligned}\beta_{L_i} &= Y_{L_i} \left[Y_{\bar{e}}^2 + \sum_j (6Y_{Q_j}^2 + 3Y_{u_j}^2 + 3Y_{d_j}^2 + 4Y_{L_j}^2 + Y_{e_j}^2) + Y^2 \right. \\ &\quad \left. - 3g_2^2 - \frac{3}{5}g_1^2 \right] + \sum_k Y_{L_k} \left(\mathbf{Y}_e^T \mathbf{Y}_e \right)_{ik},\end{aligned}\quad (\text{B.18})$$

$$\begin{aligned}\beta_{e_i} &= Y_{e_i} \left[2Y_{\bar{e}}^2 + \sum_j (6Y_{Q_j}^2 + 3Y_{u_j}^2 + 3Y_{d_j}^2 + 2Y_{L_j}^2 + 3Y_{e_j}^2) + Y^2 \right. \\ &\quad \left. - \frac{12}{5}g_1^2 \right] + \sum_k 2Y_{e_k} \left(\mathbf{Y}_e^T \mathbf{Y}_e \right)_{ik},\end{aligned}\quad (\text{B.19})$$

$$\beta_Y = 3Y \left[\sum_i (6Y_{Q_i}^2 + 3Y_{u_i}^2 + 3Y_{d_i}^2 + 2Y_{L_i}^2 + Y_{e_i}^2) + Y^2 \right]. \quad (\text{B.20})$$

References

- [1] C. Giunti, C.W. Kim and U.W. Lee, *Mod. Phys. Lett.* **A6** (1991) 1745
J. Ellis, S. Kelley and D.V. Nanopoulos, *Phys. Lett.* **260B** (1991) 131
U. Amaldi, W. de Boer and H. Fürstenau, *Phys. Lett.* **260B** (1991) 447
P. Langacker and M. Luo, *Phys. Rev.* **D44** (1991) 817
- [2] e.g. S. Raby, preprint OHSTPY-HEP-T-95-024 (hep-ph/9501349)
Z. Berezhiani, preprint INFN-FE-21-95 (hep-ph/9602325)
and references therein.
H. Arason, D.J. Castano, E.J. Piard and P. Ramond, *Phys. Rev.* **D47** (1992) 232
V. Barger, M.S. Berger and P. Ohmann, *Phys. Rev.* **D47** (1992) 1093
- [3] P. Langacker and N. Polonsky, *Phys. Rev.* **D49** (1994) 1454; *ibid.* **D50** (1994) 2199
N. Polonsky, *Phys. Rev.* **D54** (1996) 4537
- [4] M. Bando, J. Sato, T. Onogi and T. Takeuchi, *Phys. Rev.* **D56** (1997) 1589
- [5] M. Bando, J. Sato and K. Yoshioka, *Prog. Theor. Phys.* **98** (1997) 169
- [6] see for example,
M. Bando, preprint AICHI-97-3 (hep-ph/9705237) and references therein.
- [7] M.E. Peskin and T. Takeuchi, *Phys. Rev. Lett.* **65** (1990) 964; *Phys. Rev.* **D46** (1992) 381
L. Lavoura and J.P. Silva, *Phys. Rev.* **D47** (1993) 2046
N. Maekawa, *Prog. Theor. Phys.* **93** (1995) 919
- [8] K.S. Babu and J.C. Pati, *Phys. Lett.* **384B** (1996) 140
- [9] J.C. Pati, *Phys. Lett.* **228B** (1989) 228
K.S. Babu, J.C. Pati and H. Stremnitzer, *Phys. Lett.* **256B** (1991) 206; *ibid.* **264B** (1991) 347; *Phys. Rev. Lett.* **67** (1991) 1688
K.S. Babu, J.C. Pati and X. Zhang, *Phys. Rev.* **D46** (1992) 2190
K.S. Babu and J.C. Pati, *Phys. Rev.* **D48** (1993) 1921
K.S. Babu, J.C. Pati and H. Stremnitzer, *Phys. Rev.* **D51** (1995) 2451
- [10] M. Lanzagorta and G.G. Ross, *Phys. Lett.* **349B** (1995) 319
- [11] P. Ramond, R.G. Roberts and G.G. Ross, *Nucl. Phys.* **B406** (1993) 19

- [12] e.g. M. Leurer, Y. Nir and N. Seiberg, *Nucl. Phys.* **B398** (1993) 319; *ibid.* **B420** (1994) 468
P. Pouliot and N. Seiberg, *Phys. Lett.* **318B** (1993) 169
L. Ibáñez and G.G. Ross, *Phys. Lett.* **332B** (1994) 100
- [13] H. Fusaoka and Y. Koide, preprint AMU-97-02, US-97-07 (hep-ph/9712201)
- [14] Particle Data Group, *Phys. Rev.* **D54** (1996) 1
- [15] R. Gatto, G. Sartori and M. Tonin, *Phys. Lett.* **28B** (1968) 128
R.J. Oakes, *Phys. Lett.* **29B** (1969) 683
H. Fritzsch, *Nucl. Phys.* **B155** (1979) 189
- [16] D. Ng and Y.J. Ng, *Mod. Phys. Lett.* **A6** (1991) 2243
G.F. Giudice, *Mod. Phys. Lett.* **A7** (1992) 2429
W.-S. Hou and G.-G. Wong, *Phys. Rev.* **D52** (1995) 5269
- [17] T. Moroi, H. Murayama and T. Yanagida, *Phys. Rev.* **D48** (1993) 2995
B. Brahmachari, U. Sarkar and K. Sridhar, *Mod. Phys. Lett.* **A8** (1993) 3349
K. Fujikawa, *Prog. Theor. Phys.* **92** (1994) 1149
- [18] H. Fritzsch, *Phys. Lett.* **73B** (1978) 317; *Nucl. Phys.* **B155** (1979) 189
H. Georgi and D.V. Nanopoulos, *Nucl. Phys.* **B155** (1979) 52
- [19] H. Georgi and C. Jarlskog, *Phys. Lett.* **86B** (1979) 297
J.A. Harvey, P. Ramond and D.B. Reiss, *Phys. Lett.* **92B** (1980) 309
S. Dimopoulos, L.J. Hall and S. Raby, *Phys. Rev. Lett.* **68** (1992) 1984
- [20] The Muon Collider Collaboration, Fermilab-Conf-96/092, July 1996
R. Palmer, A. Tollestrup, and A. Sessler, Proc. of the 1996 DPF/DPB Summer Study on New Directions for High-energy Physics (Snowmass 96), Snowmass, CO, 25 June - 12 July 1996.